

## Article

# Feasibility of Simultaneous Multislice Acceleration Technique in Readout-Segmented Echo-Planar Diffusion-Weighted Imaging for Assessing Rectal Cancer

Mi Zhou <sup>1</sup>, Hong Pu <sup>1,\*</sup>, Mei-Ning Chen <sup>2</sup> and Yu-Ting Wang <sup>1</sup> 

<sup>1</sup> Department of Radiology, Sichuan Provincial People's Hospital, University of Electronic Science and Technology of China, Chengdu 610072, China

<sup>2</sup> Department of MR Scientific Marketing, Siemens Healthineers, Shanghai 200135, China

\* Correspondence: ph196797@163.com

**Abstract:** Background: Readout-segmented echo-planar imaging (rs-EPI) with simultaneous multislice (SMS) technology has been successfully applied to tumor research in many organs, but no feasibility study in rectal cancer has been reported, and the optimal acceleration of SMS with rs-EPI in rectal cancer has not been well determined yet. Objective: To investigate the feasibility of SMS rs-EPI of rectal cancer with different acceleration factors (AF<sub>s</sub>) and its influence on image quality, acquisition time and apparent diffusion coefficients (ADC<sub>s</sub>) in comparison to conventional sequences. Methods: All patients underwent rs-EPI and SMS rs-EPI with AF<sub>s</sub> of 2 and 3 (2 × SMS rs-EPI and 3 × SMS rs-EPI, respectively) using a 3T scanner. Acquisition times of the three rs-EPI sequences were measured. Image qualitative parameters (5-point Likert scale), signal-to-noise ratio (SNR), contrast-to-noise ratio (CNR), geometric distortion, and apparent diffusion coefficient (ADC) values of the three sequences were compared. Results: A total of eighty-three patients were enrolled in our study. rs-EPI and 2 × SMS rs-EPI offered equivalently high overall image quality with a scan time reduction to nearly half (rs-EPI: 137 s, 2 × SM rs-EPI: 60 s). 3 × SMS rs-EPI showed significantly poorer image quality ( $p < 0.05$ ). ADC values were significantly lower in 3 × SMS rs-EPI compared to rs-EPI in rectal tumors and normal tissue (tumor tissue: rs-EPI  $1.19 \pm 0.21 \times 10^{-3} \text{ mm}^2/\text{s}$ , 3 × SMS rs-EPI  $1.10 \pm 0.26 \times 10^{-3} \text{ mm}^2/\text{s}$ ,  $p < 0.001$ ; normal tissue: rs-EPI  $1.68 \pm 0.13 \times 10^{-3} \text{ mm}^2/\text{s}$ , 3 × SMS rs-EPI  $1.54 \pm 0.20 \times 10^{-3} \text{ mm}^2/\text{s}$ ,  $p < 0.001$ ). Conclusions: SMS rs-EPI using an AF of 2 is feasible for rectal MRI resulting in substantial reductions in acquisition time while maintaining diagnostic image quality and similar ADC values to those of rs-EPI when the slice distance and number of shots are the same among three rs-EPI sequences.

**Keywords:** rectal cancer; simultaneous multislice; apparent diffusion coefficient; readout-segmented echo-planar imaging



**Citation:** Zhou, M.; Pu, H.; Chen, M.-N.; Wang, Y.-T. Feasibility of Simultaneous Multislice Acceleration Technique in Readout-Segmented Echo-Planar Diffusion-Weighted Imaging for Assessing Rectal Cancer. *Diagnostics* **2023**, *13*, 474. <https://doi.org/10.3390/diagnostics13030474>

Academic Editors: Damiano Caruso and Fabiano Bini

Received: 7 September 2022

Revised: 2 January 2023

Accepted: 4 January 2023

Published: 28 January 2023



**Copyright:** © 2023 by the authors. Licensee MDPI, Basel, Switzerland. This article is an open access article distributed under the terms and conditions of the Creative Commons Attribution (CC BY) license (<https://creativecommons.org/licenses/by/4.0/>).

## 1. Introduction

Colorectal cancer is a leading cause of high morbidity and mortality worldwide, where 30–35% of colorectal cancers occur in the rectum [1,2]. Magnetic Resonance Imaging (MRI) is the preferred diagnostic tool for the local staging of rectal cancer, which provides excellent soft-tissue contrast and may be used to assess treatment response and detect postoperative local recurrence [3]. Diffusion Weighted Imaging (DWI) is a fast, non-enhanced MRI technique that does not require a contrast agent for assessing the diffusive movement of water molecules in tissues. Employing DWI with conventional MRI improves diagnostic confidence and may be used to predict rectal cancer [4,5]. Additionally, the Apparent Diffusion Coefficient (ADC) from traditional DWI provides biological implications for cell density and can identify tumor progression [6].

Due to its high speed, single-shot echo-planar imaging (ss-EPI) DWI is widely used in radiology practice, with K-space filling after a single excitation. However, due to the slow

filling along the phase-encoding direction, the low bandwidth in this direction results in blurred and distorted images. Additionally, ss-EPI is highly susceptible to magnetic field inhomogeneities and may result in geometric distortions [7]. Parallel acquisition techniques and multi-shot EPI sequences, such as readout-segmented echo-planar imaging (rs-EPI), can reduce this limitation [8]. rs-EPI divides K-space into segments along the readout direction to shorten the echo interval [8]. Previous studies have also shown that rs-EPI is superior to ss-EPI in assessing lesions in patients with rectal cancer and improving image quality; lesion conspicuity, overall image quality, geometric distortion, and distinction of anatomic structures were significantly better in rs-EPI [9].

rs-EPI, however, is limited by its long scan time, which can cause motion artifacts due to bowel peristalsis and patient discomfort. Based on the principle of simultaneously exciting multiple slices, a new method using simultaneous multislice (SMS) technology has been proposed to reduce DWI scanning time [10]. This technique involves simultaneous excitation and acquisition of multiple slices, enabling a reduction in scan time based on a greater number of simultaneously excited slices as determined by the acceleration factor (AF) [11]. In this technique, the number of slices acquired over the same pulse repetition time can be increased by setting a higher AF without the need for an increase in the gradient demand [12]. The SMS combined with DWI has been successfully applied to the kidney, liver, pancreas, breast, and other organs [13–15] with promising results. According to Park et al. [11], SMS combined with ss-EPI with an AF of 2 yields an image quality and stable ADC values comparative to those of conventional ss-EPI. In theory, image acquisition in sms-DWI can be accelerated to a large extent by increasing the applied AFs. However, an arbitrary increase of the AF is expected to come along with a deterioration of image quality [11,13]. To ascertain the optimal ratio between scan time minimization and diagnostic image quality, the use of higher AFs and the resulting image quality need to be investigated systematically. What is more, there are no studies using SMS in combination with rs-EPI in rectal cancer as far as we know, and the impact of rs-EPI combined with different SMS AFs on the image quality and ADC values of rectal cancer is also unknown.

Thus, the purpose of this study was to investigate the feasibility of SMS rs-EPI of rectal cancer with different acceleration factors (AFs) and its influence on image quality, acquisition time and apparent diffusion coefficients (ADCs) in comparison with conventional sequences.

## 2. Materials and Methods

### 2.1. Patients

This retrospective study was approved by the Institutional Review Board. Informed consent was obtained from all patients.

Based on a clinical history and physical examination results, 203 patients with clinically suspected RC were enrolled between December 2021 and June 2022. Patients with non-mucinous rectum adenocarcinoma confirmed by biopsy after endoscopically guided biopsy were included. The exclusion criteria were: (1) patients diagnosed with RC after undergoing preoperative radiotherapy and chemotherapy (n = 53); (2) tumor not visible on the MRI image (n = 14); (3) serious image artifacts, ROI measurement cannot be performed well (n = 5 for rs-EPI, n = 9 for 2 × SMS rs-EPI, n = 17 for 3 × SMS rs-EPI); (4) surgical contraindications (n = 5); (5) unresectable or metastatic diseases (n = 8); and (6) the existence of mucinous cystadenoma, whose cell density is rather low and therefore exhibits high ADC values (n = 9).

### 2.2. MRI Imaging

A 3.0T MRI scanner (MAGNETOM Vida, Siemens Healthineers, Shanghai, China) with an 18-channel body array coil was used. Bowel cleansing with enema was performed 50 min before the examination. Patients were then administered 20 mg of scopolamine butylbromide (Buscopan, Boehringer Ingelheim, Shanghai, China) intramuscularly 30 min before testing to minimize bowel motion. Three scan sequences were performed for each

subject: rs-EPI, SMS rs-EPI sequence with an acceleration factor of 2 ( $2 \times$  SMS rs-EPI), and SMS rs-EPI ( $3 \times$  SMS rs-EPI) with an acceleration factor of 3, all in free-breathing scanning mode, with the scanning direction perpendicular to the diseased intestine. Conventional MRI scan sequences were: (1) coronal breath-hold Truifi sequence (auxiliary positioning); (2) Transverse T1 VIBE DIXON sequence; and (3) Transverse high-resolution TSE T2WI sequence. The number of scanned slices was 24. The parameters of the three rs-EPI sequences are seen in Table 1. The fat press method was Spectral Attenuated Inversion Recovery (SPAIR). The b values of all DWI sequences were 0 and  $1000 \text{ s/mm}^2$  [9,16,17]. No intravenous contrast was used in this study.

**Table 1.** The parameters of three DWI sequences.

Parameters	rs-EPI	$2 \times$ SMS rs-EPI	$3 \times$ SMS rs-EPI
b value ( $\text{s/mm}^2$ )	0.1000	0.1000	0.1000
Number of Readout segments	5	5	5
Fat press method	SPAIR	SPAIR	SPAIR
TR (ms)	5000	2270	1800
TE (ms)	51	52	54
Reversal time (s)	210	210	210
FOV (mm)	$216 \times 216$	$216 \times 216$	$216 \times 216$
Matrix	$128 \times 128$	$128 \times 128$	$128 \times 128$
Voxel size ( $\text{mm}^3$ )	$1.7 \times 1.7 \times 4.5$	$1.7 \times 1.7 \times 4.5$	$1.7 \times 1.7 \times 4.5$
thickness (mm)	4.5	4.5	4.5
Distance Factor (mm)	0.45	0.45	0.45
Number of slices	24	24	24
iPAT	GRAPPA 2	GRAPPA 2	GRAPPA 2
Acceleration factor		2	3
Acquisition time (s)	137	60	51

### 2.3. Image Quality-Qualitative Analysis

All images were imported into the Syngo.via workstation, and the rs-EPI images with 2 b values were processed using the workstation's software to obtain ADC maps. All images were transferred to the picture archiving and communication system (PACS). Image analysis was independently performed by two physicians (with 6 and 16 years of diagnostic experience in MRI of the rectum, respectively) who were blinded to pathological findings and MRI sequences. Subjective parameters of image quality (lesion conspicuity, overall image quality, and margin sharpness) were evaluated based on a 5-point Likert scale, with higher scores indicating better image quality. The results of the subjective scores were averaged from the scores of the two observers. The subjective parameters were assessed in  $b = 0 \text{ s/mm}^2$ ,  $b = 1000 \text{ s/mm}^2$ , and ADC map of three rs-EPI sequences, respectively. Lesions were evaluated as follows: (1) the rectal cancer lesion was difficult to detect; (2) the lesion was minimally recognizable; (3) it was moderately visible; (4) it was well visible; (5) it showed excellent visibility. The overall image quality was evaluated as follows: (1) non-diagnostic; (2) poor; (3) satisfactory; (4) good; (5) excellent. The margin sharpness was evaluated as follows [18]: (1) not sharp; (2) slightly sharp; (3) moderately sharp; (4) good sharpness; (5) excellent sharpness [18].

### 2.4. Image Quality-Quantitative Analysis

For quantitative analysis, the two radiologists performed the region of interest (ROI) measurement in consensus. First, two ROIs were drawn on the DWI images with  $b = 0 \text{ s/mm}^2$  to include the largest possible areas of rectal cancer and normal rectal wall of the three groups, respectively. Then, the ROIs were copied to the DWI images with  $b = 1000 \text{ s/mm}^2$  for rs-EPI and SMS rs-EPI to obtain the mean signal intensity and standard deviation (Figure 1).

Signal-to-noise ratio (SNR) and contrast-to-noise (CNR) were calculated according to the following equations [19]:

$$\text{SNR} = \frac{S_{\text{lesion}}}{SD_{\text{background}}}$$

$$\text{CNR} = \frac{|S_{\text{lesion}} - S_{\text{normal tissue}}|}{\sqrt{SD_{\text{lesion}}^2 + SD_{\text{normal tissue}}^2}}$$

where  $S_{\text{lesion}}$  represents the signal intensity of the rectal mass,  $S_{\text{normal tissue}}$  represents signal intensity of the normal rectal wall, and  $SD_{\text{background}}$ ,  $SD_{\text{lesion}}$ ,  $SD_{\text{normal tissue}}$  represent the standard deviation of signal intensity of the background area, rectal mass, and normal rectal wall, respectively.

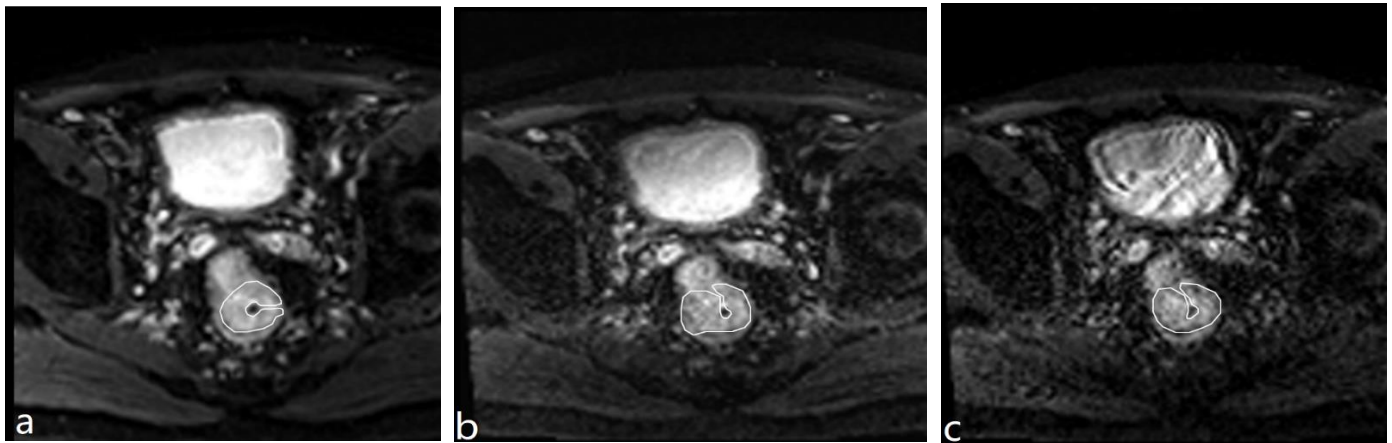


**Figure 1.** The ROI drawing for cancer lesions on the  $b = 0 \text{ s/mm}^2$  maps of rs-EPI (a);  $2 \times \text{SMS}$  rs-EPI (b),  $3 \times \text{SMS}$  rs-EPI (c).

The above quantitative parameters were measured three times to obtain the average values of the two radiologists.

The above ROI was copied onto the ADC image to measure ADC values of rectal masses. In addition, the ROI also selected the non-mass region of the rectum, and the ADC values of normal tissue were measured. The thickest level of the intestinal wall in T2WI was selected for measurement. Geometric distortion was evaluated by comparing lesion lengths in the largest areas of rectal cancer between axial T2WI images and the  $b = 0 \text{ s/mm}^2$  and  $b = 1000 \text{ s/mm}^2$  of three rs-EPI sequences. Anterior–posterior (AP) length and left–right (LR) width of the lesion were measured, and the distortion rate was calculated  $(rs - \text{EPI distance} - \text{T}_2\text{WI distance}) / \text{T}_2\text{WI distance} \times 100$  [20].

### 2.5. Statistical Analysis

SPSS version 22 (IBM Corporation) was used for analysis. Measures are expressed as  $\bar{X} \pm s$ . There was inter-reader agreement of the quantitative parameters (ADC and the qualitative image scores given by the two radiologists were assessed by calculating their respective intra-class correlation coefficients (ICC) (0.00–0.20, poor agreement; 0.21–0.40, fair agreement; 0.41–0.60, moderate agreement; 0.61–0.80, good agreement; and 0.81–1.00, excellent agreement) [21]. The Kolmogorov–Smirnov test was used to assess the normality of the quantitative data distribution. Comparisons of image quality, SNR, CNR, and geometric distortion, and the ADC values of the three groups of rs-EPI sequences were performed using the Friedman test with the Bonferroni post hoc test [11,18,22]. A  $p$  value  $< 0.05$  indicated a significant difference.

### 3. Results

Eighty-three patients (55 males and 28 females, 22–76 years old, with a mean age of  $54.6 \pm 11.9$  years old) who underwent MRI were included in this study. Results of the histochemical assay of rectal cancer were: 13 (15.7%) were well differentiated, 64 (77.1%) moderately differentiated, and 6 (7.2%) poorly differentiated. The clinicopathological features of the patients are shown in Table 2.

**Table 2.** Clinicopathological characteristics of the patients.

Clinicopathological Characteristics		<i>n</i> Percentile (%)
Gender	Male	55 (66.27)
	Female	28 (33.73)
Age (years)		58.82 (11.71)
BMI ( $\text{kg}\cdot\text{m}^{-2}$ )		22.82 (1.91)
Location of tumor	Upper-middle segment	34 (40.96)
	Lower segment	49 (59.04)
differentiation grade	well	13 (15.7)
	moderate	64 (77.1)
	poor	6 (7.2)
CEA	+	55 (66.27)
	–	28 (33.73)
CA19-9	+	40 (48.19)
	–	43 (51.81)
Nerve invasion	+	56 (67.5)
	–	27 (32.5)
Vascular cancer embolus	+	61 (73.5)
	–	22 (26.5)
Cancer nodules	+	68 (81.9)
	–	15 (18.1)

#### 3.1. Acquisition Time

The scanning time of  $2 \times \text{SMS rs-EPI}$  was 60 s, which was 56.2% shorter than that of 137 s for rs-EPI sequences; the scanning time of  $3 \times \text{SMS rs-EPI}$  was 51 s, which was 72.8% shorter than that of rs-EPI sequences.

#### 3.2. Qualitative Analysis

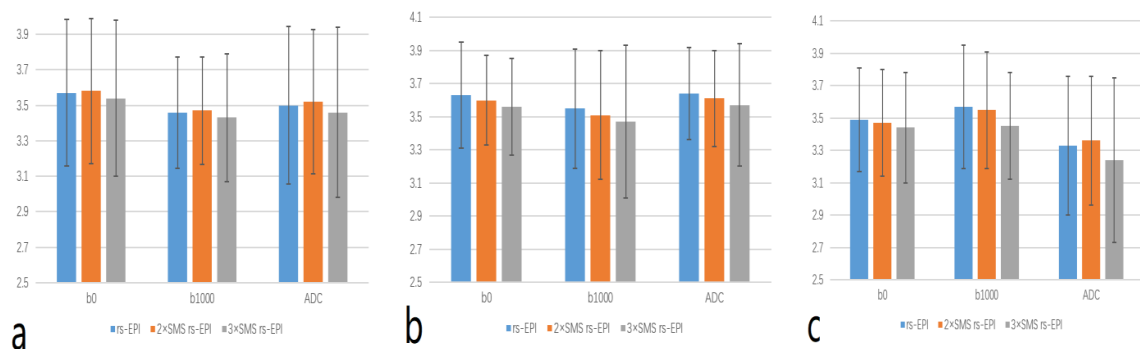
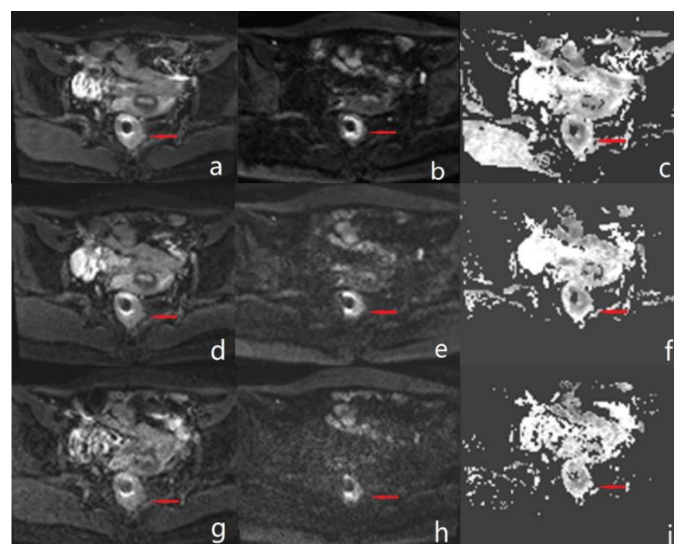
The inter-reader agreement was excellent for lesion conspicuity (ICC = 0.843 (0.763–0.896), 0.947 (0.919–0.965) and 0.772 (0.669–0.846)), overall image quality (ICC = 0.895 (0.842–0.931), 0.847 (0.773–0.898) and 0.844 (0.768–0.896)), margin sharpness (ICC = 0.929 (0.891–0.954), 0.935 (0.901–0.957) and 0.942 (0.912–0.962)) in rs-EPI,  $2 \times \text{SMS rs-EPI}$  and  $3 \times \text{SMS rs-EPI}$ , respectively.

The scores of lesion conspicuity, overall image quality and margin sharpness on DWI images and ADC map were significantly different among rs-EPI,  $2 \times \text{SMS rs-EPI}$ , and  $3 \times \text{SMS rs-EPI}$  ( $p < 0.05$ ), while there were no significant different between  $2 \times \text{SMS rs-EPI}$  and rs-EPI (all  $p > 0.05$ ). In the  $b = 1000 \text{ s}/\text{mm}^2$  DWI image of the  $3 \times \text{SMS rs-EPI}$  sequence, parallel acquisition artifacts can be seen, and rectal structures were poorly visualized (Table 3 and Figures 2 and 3).

**Table 3.** Comparison of three rs-EPI sequences showing subjective scores of rectal image quality.

Qualitative Parameters	rs-EPI	2 × SMS rs-EPI	3 × SMS rs-EPI	X <sup>2</sup> Value	p-Value
<b>Lesion Conspicuity</b>					
b = 0 s/mm <sup>2</sup>	3.57 ± 0.41	3.58 ± 0.41	3.54 ± 0.44 <sup>ab</sup>	11.143	0.004
b = 1000 s/mm <sup>2</sup>	3.46 ± 0.31	3.47 ± 0.30	3.43 ± 0.36 <sup>ab</sup>	9.579	0.008
ADC map (×10 <sup>-3</sup> mm <sup>2</sup> /s)	3.50 ± 0.44	3.52 ± 0.41	3.46 ± 0.48 <sup>ab</sup>	6.909	0.032
<b>Overall image quality</b>					
b = 0 s/mm <sup>2</sup>	3.63 ± 0.32	3.60 ± 0.27	3.56 ± 0.29 <sup>ab</sup>	9.579	0.008
b = 1000 s/mm <sup>2</sup>	3.55 ± 0.36	3.51 ± 0.39	3.47 ± 0.46 <sup>ab</sup>	11.273	0.004
ADC map (×10 <sup>-3</sup> mm <sup>2</sup> /s)	3.64 ± 0.28	3.61 ± 0.29	3.57 ± 0.37 <sup>ab</sup>	11.273	0.004
<b>Margin sharpness</b>					
b = 0 s/mm <sup>2</sup>	3.49 ± 0.32	3.47 ± 0.33	3.44 ± 0.34	18.488	<0.001
b = 1000 s/mm <sup>2</sup>	3.57 ± 0.38	3.55 ± 0.36	3.45 ± 0.33 <sup>ab</sup>	14.392	0.001
ADC map (×10 <sup>-3</sup> mm <sup>2</sup> /s)	3.33 ± 0.43	3.36 ± 0.40	3.24 ± 0.51 <sup>ab</sup>	18.588	<0.001

Note: <sup>a</sup> compared with rs-EPI,  $p < 0.05$ ; <sup>b</sup> compared with 2 × SMS rs-EPI,  $p < 0.05$ .

**Figure 2.** Comparison of qualitative evaluation metrics of the three EPI sequences. (a) lesion conspicuity; (b) overall image quality; (c) margin sharpness.**Figure 3.** Male, 53 years old with rectal cancer. (a–c) Diffusion-weighted and ADC maps of conventional rs-EPI sequences with b-values of 0 s/mm<sup>2</sup> and 1000 s/mm<sup>2</sup>, respectively. (d–f) Diffusion-weighted and ADC maps of 2 × SMS rs-EPI sequences with b-values of 0 s/mm<sup>2</sup> and 1000 s/mm<sup>2</sup>, respectively. (g–i) Diffusion-weighted and ADC maps of 3 × SMS rs-EPI sequences with b-values of 0 s/mm<sup>2</sup> and 1000 s/mm<sup>2</sup>, respectively. The arrow in the figure points to a rectal cancer lesion.

### 3.3. Quantitative Image Quality Analysis

The SNR and CNR on DWI images were significantly different among three rs-EPI sequences (all  $p < 0.001$ ), while these were not significantly different between  $2 \times$  SMS rs-EPI and rs-EPI (all  $p > 0.001$ ). Geometric distortions on DWI images were statistically different among the three groups of sequences and the geometric distortion of  $2 \times$  SMS rs-EPI was the lowest (Table 4).

**Table 4.** Comparison of quantitative evaluation indexes of three EPI sequences.

	Rs-EPI	$2 \times$ SMS rs-EPI	$3 \times$ SMS rs-EPI	$X^2$ Value	$p$ Value
SNR					
$b = 0 \text{ s/mm}^2$	$120.95 \pm 21.66$	$119.52 \pm 23.27$	$111.88 \pm 19.31^{ab}$	36.105	<0.001
$b = 1000 \text{ s/mm}^2$	$53.31 \pm 7.15$	$52.79 \pm 7.58$	$52.42 \pm 8.09^{ab}$	13.040	0.001
CNR					
$b = 0 \text{ s/mm}^2$	$4.84 \pm 0.47$	$4.88 \pm 0.47$	$4.74 \pm 0.55^{ab}$	32.109	<0.001
$b = 1000 \text{ s/mm}^2$	$4.26 \pm 0.67$	$4.31 \pm 0.67$	$4.18 \pm 0.75^{ab}$	18.588	<0.001
Geometric distortion					
$b = 0 \text{ s/mm}^2$	$3.49 \pm 0.32$	$3.47 \pm 0.32$	$3.51 \pm 0.33^{ab}$	13.231	0.001
$b = 1000 \text{ s/mm}^2$	$3.57 \pm 0.38$	$3.52 \pm 0.33$	$3.61 \pm 0.43^{ab}$	25.529	<0.001

Note: <sup>a</sup> compared with rs-EPI,  $p < 0.05$ ; <sup>b</sup> compared with  $2 \times$  SMS rs-EPI,  $p < 0.05$ .

The inter-observer agreement was excellent for  $ADC_{\text{lesion}}$  (ICC = 0.931 (0.895, 0.955), 0.963 (0.942, 0.976), and 0.854 (0.775, 0.906)) for rs-EPI,  $2 \times$  SMS rs-EPI, and  $3 \times$  SMS rs-EPI, respectively. The inter-observer agreement was excellent for  $ADC_{\text{normalized}}$  (ICC = 0.889 (0.825, 0.930), 0.885 (0.760, 0.938), and 0.854 (0.775, 0.906)) for rs-EPI,  $2 \times$  SMS rs-EPI, and  $3 \times$  SMS rs-EPI, respectively.

In the comparison between rectal tumor tissues of ADC values, there was a significant difference among three rs-EPI sequences ( $1.19 \pm 0.21$  vs.  $1.18 \pm 0.22$  vs.  $1.10 \pm 0.26$ ,  $p < 0.001$ ). In the comparison between rectal normal tissues of ADC values, there was a significant difference among three rs-EPI sequences ( $1.68 \pm 0.13$  vs.  $1.66 \pm 0.14$  vs.  $1.54 \pm 0.20$ ,  $p < 0.001$ ). For rectal tumor tissue and normal rectal tissue, there were no significant differences between the  $2 \times$  SMS rs-EPI and rs-EPI sequences ( $p = 0.068/p = 0.066$ ); There was a significant difference of ADC values between  $3 \times$  SMS rs-EPI and  $2 \times$  SMS rs-EPI,  $3 \times$  SMS rs-EPI and rs-EPI (all  $p < 0.001$ ). With the increase of the acceleration factor, the ADC values of both normal rectal tissue and tumor tissue decreased, as shown in Table 5 and Figure 4.

**Table 5.** The comparison of ADC value between three EPI sequences.

	rs-EPI	$2 \times$ SMS rs-EPI	$3 \times$ SMS rs-EPI	$X^2$ Value	$p$ Value
$ADC_{\text{Lesion}} (10^{-3} \text{ mm}^2/\text{s})$	$1.19 \pm 0.21$	$1.18 \pm 0.22$	$1.10 \pm 0.26^{ab}$	40.582	<0.001
$ADC_{\text{Normalized}} (10^{-3} \text{ mm}^2/\text{s})$	$1.68 \pm 0.13$	$1.66 \pm 0.14$	$1.54 \pm 0.20^{ab}$	51.835	<0.001

Note: <sup>a</sup> compared with rs-EPI,  $p < 0.05$ ; <sup>b</sup> compared with  $2 \times$  SMS rs-EPI,  $p < 0.05$ .

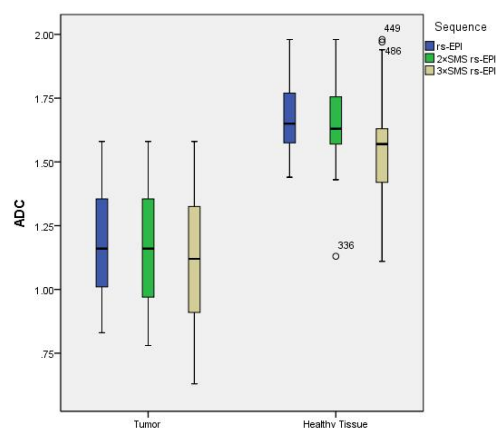


**Figure 4.** Box plot of the differences between ADC values ( $10^{-3} \text{ mm}^2/\text{s}$ ) in tumors and healthy tissue measured using the three sequences.

#### 4. Discussion

Our study found that, using an AF of 2,  $2 \times \text{SMS rs-EPI}$  allowed for a considerable reduction of acquisition time while maintaining high diagnostic image quality and lesion conspicuity. When increasing the AF to 3, a significant deterioration in image quality was observed in patients with reduced visibility of all organ parts in the diffusion weighted images and reduced image quality of the corresponding ADC maps. Moreover, artefacts and signal inhomogeneity in  $3 \times \text{SMS rs-EPI}$  were significantly increased, which led to a poorer overall image quality and to a limited lesion conspicuity, thus discarding the use of higher AFs for clinical routine applications in its current implementation. Based on these results, further evaluation of AFs higher than 3 was waived.

The scan acquisition time can be accelerated by increasing the acceleration factor of SMS, while an excessive acceleration factor is expected to be accompanied by a deterioration in image quality. Therefore, the most important thing is to find the balance between shortening the scanning time by SMS AFs and obtaining the best image quality. In our study, we found that  $2 \times \text{SMS rs-EPI}$  can reduce the scanning time while obtaining better image quality, since there was no difference in scores of overall image quality, lesion conspicuity, and margin sharpness of the DWI images and ADC map compared with rs-EPI. These results are the same as those previously reported [11,18,19]. Neither the parotid gland tumors nor nasopharyngeal carcinoma were affected by the significant motion of the organ, and a better image quality can be obtained using  $2 \times \text{SMS rs-EPI}$ , but the rectum is more affected by intestinal peristalsis;  $2 \times \text{SMS rs-EPI}$  can still obtain stable, high-quality images. However, a significantly worse overall image quality was observed, for lesion conspicuity and margin sharpness, between  $3 \times \text{SMS rs-EPI}$  and the other two sequences. SMS acceleration includes acceleration factor phase encoding (PE) and SMS factor. Excessive SMS acceleration factor reduced the intra-slice SNR, making it impossible for the GRAPPA algorithm used in acceleration factor PE to decode the parallel acquired data and create artifacts. Therefore, although an acceleration factor of 3 can significantly reduce the scan time, it is not feasible in rectal applications.

Tu, C et al. [18] compared the CNR and lesion distortion between rs-EPI,  $2 \times \text{SMS rs-EPI}$  and  $3 \times \text{SMS rs-EPI}$  in 105 nasopharyngeal carcinomas and reported that no significant differences were found in the CNR and lesion distortion between rs-EPI and  $2 \times \text{SMS rs-EPI}$ ; however, the  $3 \times \text{SMS rs-EPI}$  shows the lowest CNR and lesion distortion. In this study, we found similar CNR but less geometric distortion in  $2 \times \text{SMS rs-EPI}$  vs. rs-EPI, similar to Jiang et al.'s study [19]. It is important to reduce distortion in rectal cancer MR imaging, and a true rectal display helps us to observe the circumferential resection margin (CRM) status, epidural vascular invasion (EMVI), depth of epidural invasion (EVI), discontinuous epidural vascular spread/deposition, and mucus presence; besides the T and N stages, these high-risk features also facilitate clinical decision making and can be

used to classify rectal cancer patients according to their prognosis [23,24]. Our study result indicated that the SMS technique with an acceleration factor of 2 reduces the scan time without compromising image quality and with less distortion in the rectum, which can increase the clinical usability of rs-EPI for assessing rectal cancers.

The ADC values of rectal cancer may reflect cancer aggressiveness, which can predict the histologic T stage, differentiation, and therapeutic response after chemoradiotherapy [25]. Several studies reported no significant differences in ADC values between  $2 \times$  SMS ss-EPI and conventional ss-EPI in several organs [26–28], including the rectum [11]. Our study also revealed that there was no significant difference of ADC values between rs-EPI and  $2 \times$  SMS rs-EPI in the tumor tissue and normal tissue of the rectal cancer. A few previous studies have reported decreased ADC values using SMS-DWI in the liver and pancreas in comparison with conventional DWI [15,22,29,30]. These studies hypothesized that the elevated noise floor in SMS-DWI may result in generally lower ADC values [22]. However, several subsequent studies reported no significant differences in ADC values between SMS-accelerated sequences and conventional DWI in several organs [26–28], which is in line with our results. This difference may be explained by the fact that the TR was chosen to be as low as possible to minimize SMS technology, resulting in a lower SNR of DWI images and unstable calculated ADC values [22,30].

Our study had limitations. First, this was a retrospective, single-center study with a small sample size. Second, the study population included only patients with biopsy-confirmed rectal cancer, while further studies should include patients with benign rectal lesions or those who received radiotherapy for rectal cancer to validate the study findings further. Third, manual human measurement of ROI values increases the likelihood of sample error. Fourth, our study only examines the acceleration factor and does not discuss the impact of slice distance and number of shots on image quality, it will be designed and added prospectively in subsequent studies.

## 5. Conclusions

SMS rs-EPI using an AF of 2 is feasible for rectal MRI resulting in substantial reductions in acquisition time while maintaining diagnostic image quality and similar ADC values to those of rs-EPI when the slice distance and number of shots are the same among three rs-EPI sequences.

**Author Contributions:** Conceptualization, M.Z. and Y.-T.W.; methodology, M.-N.C.; software, M.-N.C.; formal analysis, H.P.; writing—original draft preparation, M.Z.; writing—review and editing, H.P. and Y.-T.W.; All authors have read and agreed to the published version of the manuscript.

**Funding:** This research received no external funding.

**Institutional Review Board Statement:** The study was conducted in accordance with the Declaration of Helsinki, and was approved by the Institutional Review Board of Sichuan Provincial People's hospital, University of Electronic Science and Technology of China. NO: Lun Audit (Research) No. 86 of 2021, dated 1 March 2021).

**Informed Consent Statement:** Informed consent was obtained from all subjects involved in the study.

**Data Availability Statement:** The data is unavailable due to privacy or ethical restrictions.

**Conflicts of Interest:** The authors declare no conflict of interest.

## References

1. Asgeirsson, T.; Zhang, S.; Senagore, A.J. Optimal follow-up to curative colon and rectal cancer surgery: How and for how long? *Surg. Oncol. Clin. N. Am.* **2010**, *19*, 861–873. [[CrossRef](#)] [[PubMed](#)]
2. Lee, Y.C.; Hsieh, C.C.; Chuang, J.P. Prognostic significance of partial tumor regression after preoperative chemoradiotherapy for rectal cancer: A meta-analysis. *Dis. Colon. Rectum* **2013**, *56*, 1093–1101. [[CrossRef](#)] [[PubMed](#)]
3. Fernandes, M.C.; Gollub, M.J.; Brown, G. The importance of MRI for rectal cancer evaluation. *Surg. Oncol.* **2022**, *43*, 101739. [[CrossRef](#)]

4. Kim, S.H.; Lee, J.M.; Hong, S.H.; Kim, G.H.; Lee, J.Y.; Han, J.K.; Choi, B.I. Locally advanced rectal cancer: Added value of diffusion-weighted MR imaging in the evaluation of tumor response to neoadjuvant chemo- and radiation therapy. *Radiology* **2009**, *253*, 116–125. [[CrossRef](#)] [[PubMed](#)]
5. Beets-Tan, R.G.H.; Lambregts, D.M.J.; Maas, M.; Bipat, S.; Barbaro, B.; Curvo-Semedo, L.; Fenlon, H.M.; Gollub, M.J.; Gourtsoyianni, S.; Halligan, S.; et al. Magnetic resonance imaging for clinical management of rectal cancer: Updated recommendations from the 2016 European Society of Gastrointestinal and Abdominal Radiology (ESGAR) consensus meeting. *Eur. Radiol.* **2018**, *28*, 1465–1475. [[CrossRef](#)]
6. Geng, Z.; Zhang, Y.; Yin, S.; Lian, S.; He, H.; Li, H.; Xie, C.; Dai, Y. Preoperatively Grading Rectal Cancer with the Combination of Intravoxel Incoherent Motions Imaging and Diffusion Kurtosis Imaging. *Contrast Media Mol. Imaging* **2020**, *2020*, 2164509. [[CrossRef](#)] [[PubMed](#)]
7. Birlik, B.; Obuz, F.; Elibol, F.D.; Celik, A.O.; Sokmen, S.; Terzi, C.; Sagol, O.; Sarioglu, S.; Gorken, I.; Oztop, I. Diffusion-weighted MRI and MR- volumetry—in the evaluation of tumor response after preoperative chemoradiotherapy in patients with locally advanced rectal cancer. *Magn. Reson. Imaging* **2015**, *33*, 201–212. [[CrossRef](#)]
8. Porter, D.A.; Heidemann, R.M. High resolution diffusion-weighted imaging using readout-segmented echo-planar imaging, parallel imaging and a two-dimensional navigator-based reacquisition. *Magn. Reson. Med.* **2009**, *62*, 468–475. [[CrossRef](#)]
9. Xia, C.C.; Liu, X.; Peng, W.L.; Li, L.; Zhang, J.G.; Meng, W.J.; Deng, X.B.; Zuo, P.L.; Li, Z.L. Readout-segmented echo-planar imaging improves the image quality of diffusion-weighted MR imaging in rectal cancer: Comparison with single-shot echo-planar diffusion-weighted sequences. *Eur. J. Radiol.* **2016**, *85*, 1818–1823. [[CrossRef](#)]
10. Moeller, S.; Yacoub, E.; Olman, C.A.; Auerbach, E.; Strupp, J.; Harel, N.; Ugurbil, K. Multiband multislice GE-EPI at 7 tesla, with 16-fold acceleration using partial parallel imaging with application to high spatial and temporal whole-brain fMRI. *Magn. Reson. Med.* **2010**, *63*, 1144–1153. [[CrossRef](#)]
11. Park, J.H.; Seo, N.; Lim, J.S.; Hahm, J.; Kim, M.J. Feasibility of Simultaneous Multislice Acceleration Technique in Diffusion-Weighted Magnetic Resonance Imaging of the Rectum. *Korean J. Radiol.* **2020**, *21*, 77–87. [[CrossRef](#)] [[PubMed](#)]
12. Xu, J.; Moeller, S.; Auerbach, E.J.; Strupp, J.; Smith, S.M.; Feinberg, D.A.; Yacoub, E.; Ugurbil, K. Evaluation of slice accelerations using multiband echo planar imaging at 3 T. *NeuroImage* **2013**, *83*, 991–1001. [[CrossRef](#)] [[PubMed](#)]
13. Koeter, T.; Jongen, G.; Hanrath-Vos, E.; Smit, E.; Futterer, J.; Maas, M.; Scheenen, T. Reducing Acquisition Time of Diffusion Weighted MR Imaging of the Rectum with Simultaneous Multi-Slice Acquisition: A Reader Study. *Acad. Radiol.* **2022**, *29*, 1802–1807. [[CrossRef](#)] [[PubMed](#)]
14. Song, S.E.; Woo, O.H.; Cho, K.R.; Seo, B.K.; Son, Y.H.; Grimm, R.; Liu, W.; Moon, W.K. Simultaneous Multislice Readout-Segmented Echo Planar Imaging for Diffusion-Weighted MRI in Patients with Invasive Breast Cancers. *J. Magn. Reson. Imaging* **2021**, *53*, 1108–1115. [[CrossRef](#)]
15. Obele, C.C.; Glielmi, C.; Ream, J.; Doshi, A.; Campbell, N.; Zhang, H.C.; Babb, J.; Bhat, H.; Chandarana, H. Simultaneous Multislice Accelerated Free-Breathing Diffusion-Weighted Imaging of the Liver at 3 T. *Abdom. Imaging* **2015**, *40*, 2323–2330. [[CrossRef](#)]
16. Lambregts, D.M.J.; van Heeswijk, M.M.; Delli Pizzi, A.; van Elderen, S.G.C.; Andrade, L.; Peters, N.; Kint, P.A.M.; Osinga-de Jong, M.; Bipat, S.; Ooms, R.; et al. Diffusion-weighted MRI to assess response to chemoradiotherapy in rectal cancer: Main interpretation pitfalls and their use for teaching. *Eur. Radiol.* **2017**, *27*, 4445–4454. [[CrossRef](#)]
17. Chen, Y.; Jiang, Z.; Guan, X.; Li, H.; Li, C.; Tang, C.; Lei, Y.; Dang, Y.; Song, B.; Long, L. The value of multi-parameter diffusion and perfusion magnetic resonance imaging for evaluating epithelial-mesenchymal transition in rectal cancer. *Eur. J. Radiol.* **2022**, *150*, 110245. [[CrossRef](#)]
18. Tu, C.; Shen, H.; Liu, D.; Chen, Q.; Yuan, X.; Li, X.; Wang, X.; Liu, R.; Wang, X.; Li, Q.; et al. Simultaneous multi-slice readout-segmentation of long variable echo-trains for accelerated diffusion-weighted imaging of nasopharyngeal carcinoma: A feasibility and optimization study. *Clin. Imaging* **2021**, *79*, 119–124. [[CrossRef](#)]
19. Jiang, J.S.; Zhu, L.N.; Wu, Q.; Sun, Y.; Liu, W.; Xu, X.Q.; Wu, F.Y. Feasibility study of using simultaneous multi-slice RESOLVE diffusion weighted imaging to assess parotid gland tumors: Comparison with conventional RESOLVE diffusion weighted imaging. *BMC Med. Imaging* **2020**, *20*, 93. [[CrossRef](#)] [[PubMed](#)]
20. Hirata, K.; Nakaura, T.; Okuaki, T.; Kidoh, M.; Oda, S.; Utsunomiya, D.; Namimoto, T.; Kitajima, M.; Nakayama, H.; Yamashita, Y. Comparison of the image quality of turbo spin echo- and echo-planar diffusion-weighted images of the oral cavity. *Medicine* **2018**, *97*, e0447. [[CrossRef](#)]
21. Peng, Y.; Li, Z.; Tang, H.; Wang, Y.; Hu, X.; Shen, Y.; Hu, D. Comparison of reduced field-of-view diffusion-weighted imaging (DWI) and conventional DWI techniques in the assessment of rectal carcinoma at 3.0T: Image quality and histological T staging. *J. Magn. Reson. Imaging* **2018**, *47*, 967–975. [[CrossRef](#)] [[PubMed](#)]
22. Taron, J.; Martirosian, P.; Kuestner, T.; Schwenzler, N.F.; Othman, A.; Weiß, J.; Notohamiprodjo, M.; Nikolaou, K.; Schraml, C. Scan time reduction in diffusion-weighted imaging of the pancreas using a simultaneous multislice technique with different acceleration factors: How fast can we go? *Eur. Radiol.* **2018**, *28*, 1504–1511. [[CrossRef](#)] [[PubMed](#)]
23. Yang, Y.S.; Qiu, Y.J.; Zheng, G.H.; Gong, H.P.; Ge, Y.Q.; Zhang, Y.F.; Feng, F.; Wang, Y.T. High resolution MRI-based radiomic nomogram in predicting perineural invasion in rectal cancer. *Cancer Imaging* **2021**, *21*, 40. [[CrossRef](#)] [[PubMed](#)]
24. Yang, Y.S.; Feng, F.; Qiu, Y.J.; Zheng, G.H.; Ge, Y.Q.; Wang, Y.T. High-resolution MRI-based radiomics analysis to predict lymph node metastasis and tumor deposits respectively in rectal cancer. *Abdom. Radiol.* **2021**, *46*, 873–884. [[CrossRef](#)]

25. Choi, M.H.; Oh, S.N.; Rha, S.E.; Choi, J.I.; Lee, S.H.; Jang, H.S.; Kim, J.G.; Grimm, R.; Son, Y. Diffusion-weighted imaging: Apparent diffusion coefficient histogram analysis for detecting pathologic complete response to chemoradiotherapy in locally advanced rectal cancer. *J. Magn. Reson. Imaging* **2016**, *44*, 212–220. [[CrossRef](#)] [[PubMed](#)]
26. Kenkel, D.; Barth, B.K.; Piccirelli, M.; Filli, L.; Finkenstädt, T.; Reiner, C.S.; Boss, A. Simultaneous Multislice Diffusion-Weighted Imaging of the Kidney: A Systematic Analysis of Image Quality. *Investig. Radiol.* **2017**, *52*, 163–169. [[CrossRef](#)]
27. Taron, J.; Weiß, J.; Martirosian, P.; Seith, F.; Stemmer, A.; Bamberg, F.; Notohamiprodjo, M. Clinical Robustness of Accelerated and Optimized Abdominal Diffusion-Weighted Imaging. *Investig. Radiol.* **2017**, *52*, 590–595. [[CrossRef](#)]
28. Weiss, J.; Martirosian, P.; Taron, J.; Othman, A.E.; Kuestner, T.; Erb, M.; Bedke, J.; Bamberg, F.; Nikolaou, K.; Notohamiprodjo, M. Feasibility of accelerated simultaneous multislice diffusion-weighted MRI of the prostate. *J. Magn. Reson. Imaging* **2017**, *46*, 1507–1515. [[CrossRef](#)] [[PubMed](#)]
29. Boss, A.; Barth, B.; Filli, L.; Kenkel, D.; Wurnig, M.C.; Piccirelli, M.; Reiner, C.S. Simultaneous multi-slice echo planar diffusion weighted imaging of the liver and the pancreas: Optimization of signal-to-noise ratio and acquisition time and application to intravoxel incoherent motion analysis. *Eur. J. Radiol.* **2016**, *85*, 1948–1955. [[CrossRef](#)]
30. Taron, J.; Martirosian, P.; Erb, M.; Kuestner, T.; Schwenzler, N.F.; Schmidt, H.; Honndorf, V.S.; Weiß, J.; Notohamiprodjo, M.; Nikolaou, K.; et al. Simultaneous multislice diffusion-weighted MRI of the liver: Analysis of different breathing schemes in comparison to standard sequences. *J. Magn. Reson. Imaging* **2016**, *44*, 865–879. [[CrossRef](#)]

**Disclaimer/Publisher’s Note:** The statements, opinions and data contained in all publications are solely those of the individual author(s) and contributor(s) and not of MDPI and/or the editor(s). MDPI and/or the editor(s) disclaim responsibility for any injury to people or property resulting from any ideas, methods, instructions or products referred to in the content.